Search for Standard Model Higgs boson in taus at CMS

Raman Khurana

On behalf of
CMS
Colloboration

HIGGS
&
BEYOND THE STANDARD MODEL
PHYSICS AT LHC
24^{th} – 28^{th} June 2013

Motivation

- High σ x BR at low masses.
- Sensitive to all Higgs production modes.
- Probe direct coupling to leptons

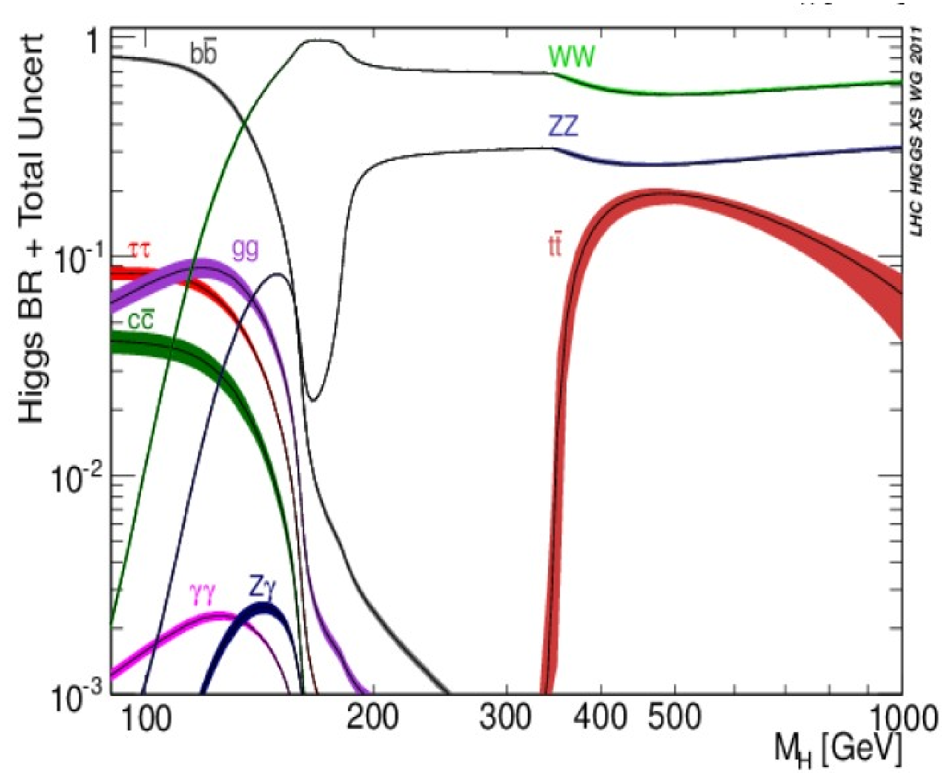

At M_H = 125GeV

19.52pb^{-1}

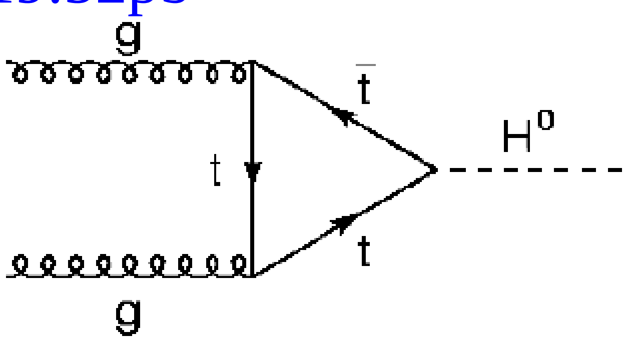

gluon gluon production

1.578 pb^{-1}

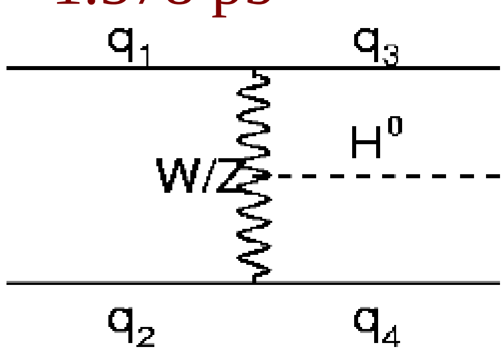

Vector boson fusion production

0.6966 (0.3943) pb^{-1} for WH(ZH)

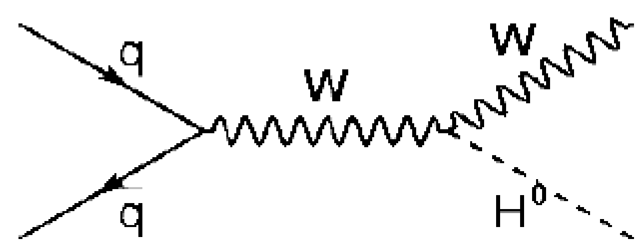

Associated Higgs production

The CMS Detector

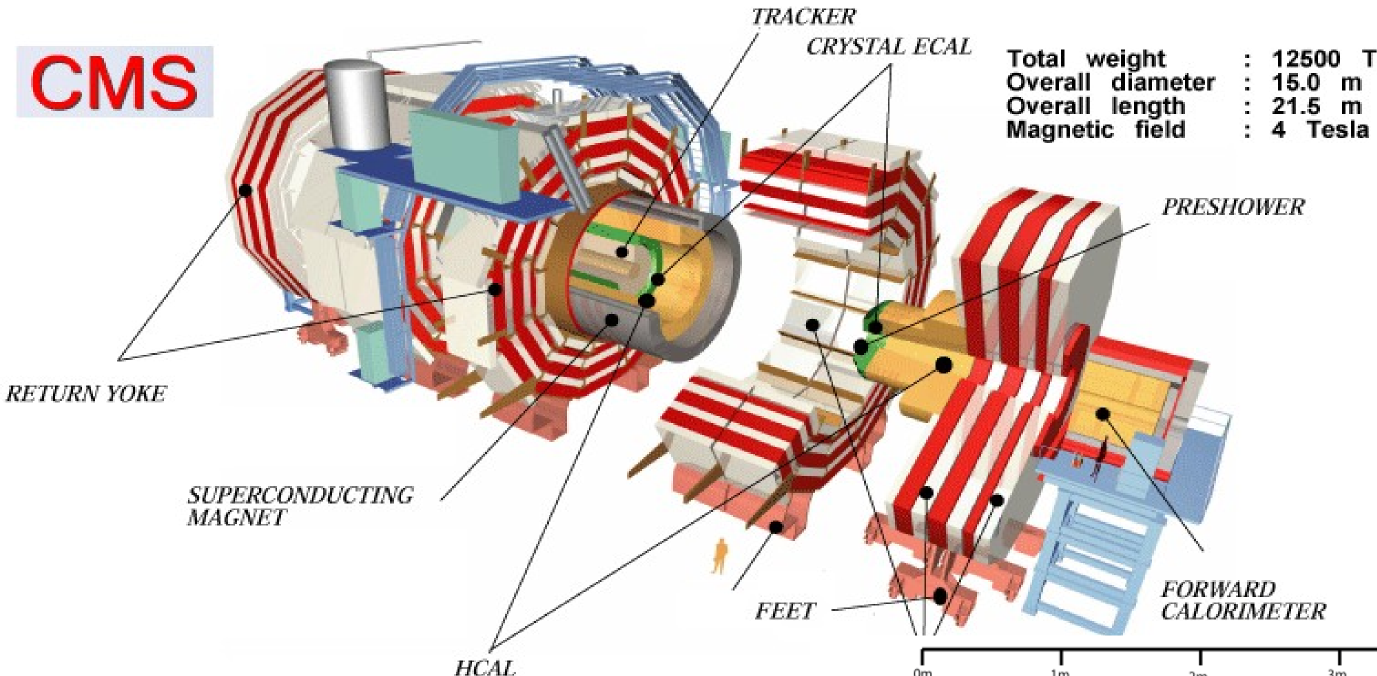

- General purpose detector to study physics at LHC
- Subdetectors in form of concentric cylinders
  - Silicon Tracker (Pixel+Strips)
  - Calorimeters (ECAL+HCAL)
  - Magnet
  - Muon System

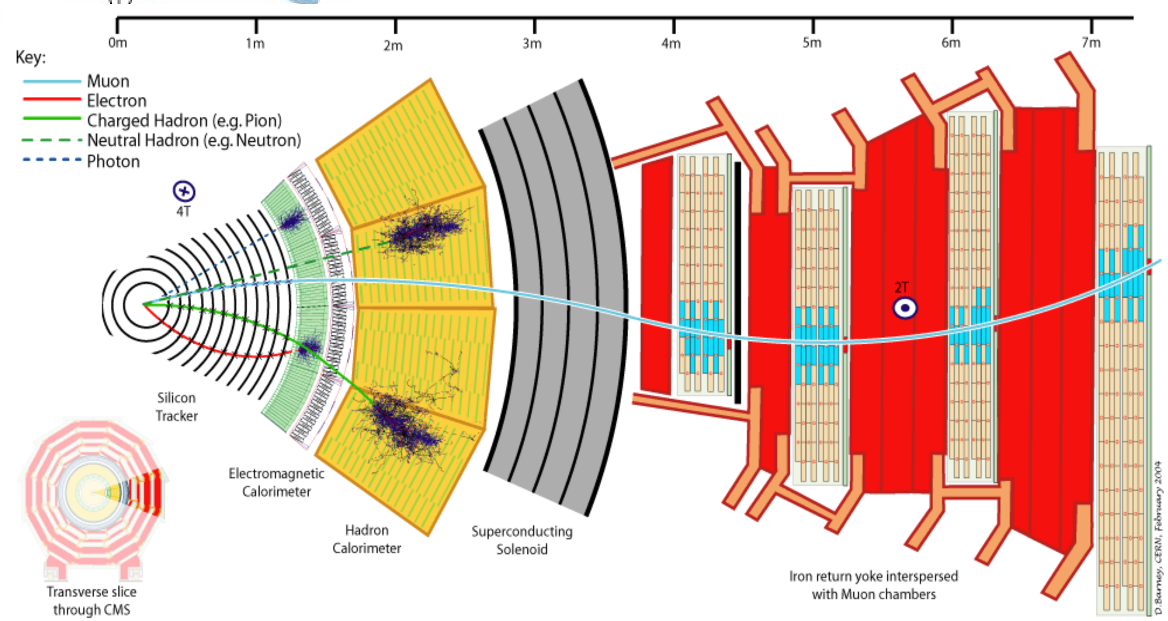

Tau reconstruction : Hadron Plus Strips (HPS)

- CMS uses particle flow algorithm (which exploits information of all sub-detectors) to identify & reconstruct particles namely charged hadron, e, mu, neutral hadron, gamma.
- The resulting list of particles are used to reconstruct hadronic taus using an algorithm named Hadron Plus Strips (HPS).
- Visible product of hadronic tau decays are used to reconstruct the taus.
- Major task of the HPS algorithm is to determine the number of π^0 in the decay.

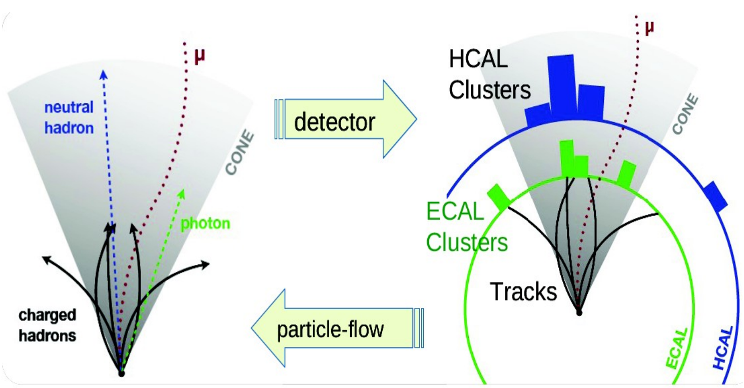

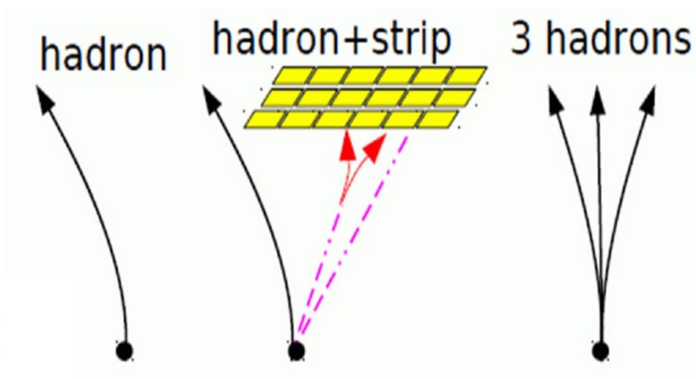

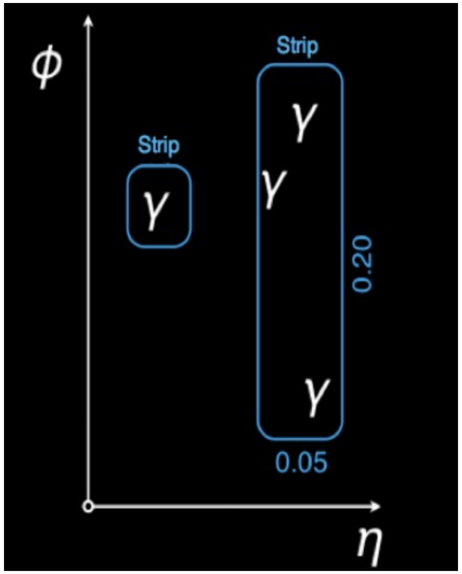

- It combined PF electromagnetic particles in the strip, to take care possible broadening of calorimetric deposition because of photon conversion.
- The neutral objects are then combined with existing charged hadrons to reconstruct hadronic tau.
- To differentiate τ_h from ordinary gluon or quark jets isolation criteria is used.
- The isolation requires that there are no charged hadron or photon apart from τ_h decay product around τ_h.

Tau reconstruction : Performance

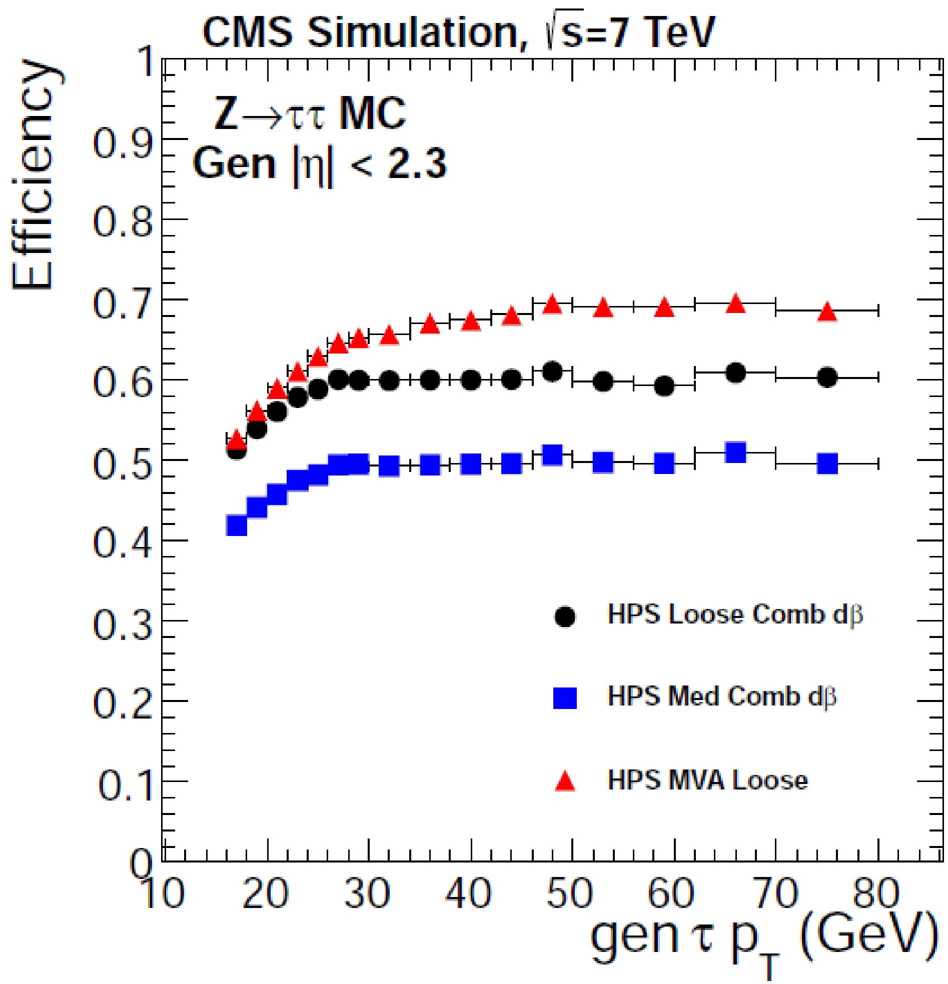

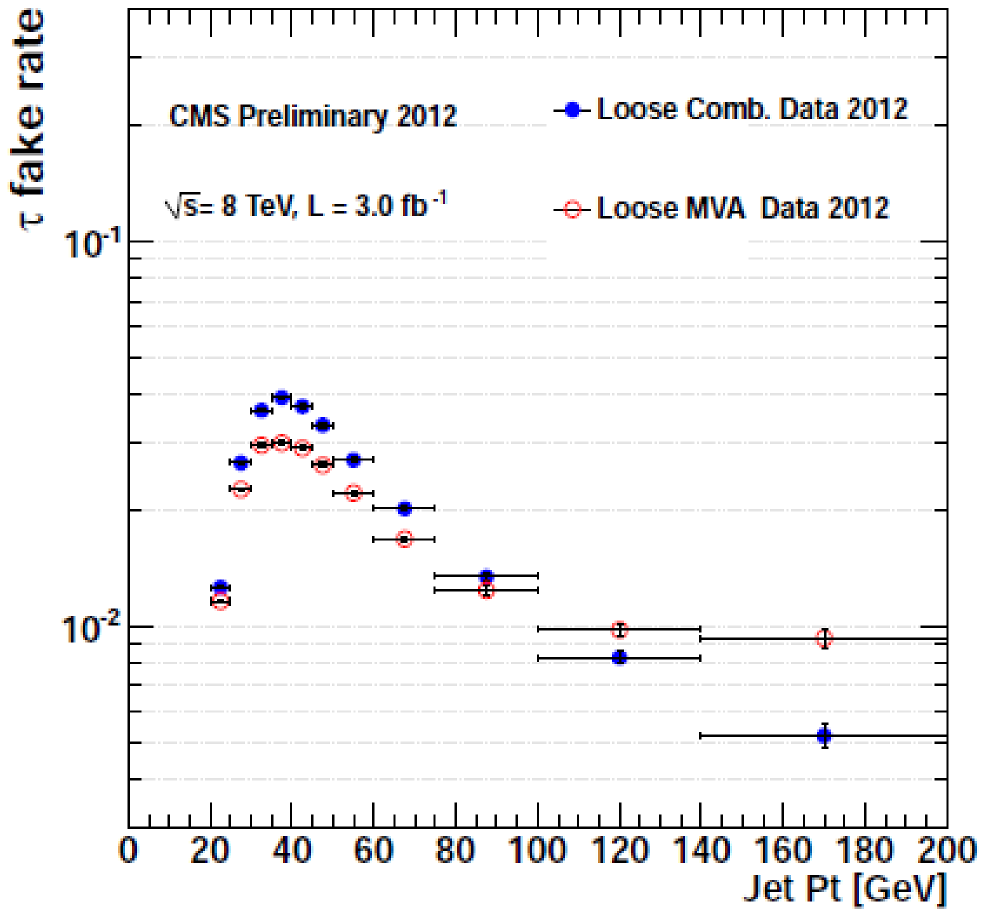

- Tau efficiency flat vs. p_T after ~25 GeV
- Fake rate ~3% for a τ_h efficiency of ~65%.

MET : Performance

CMS PAS JME-12-002

- Resolution of PF E_T^{miss} degrades rapidly with number of pile up interactions.
- E_T^{miss} resolution estimated from recoil against Z boson.
  - $U_{||}$: parallel component of recoil
  - $U_{\perp}$: perpendicular component of recoil

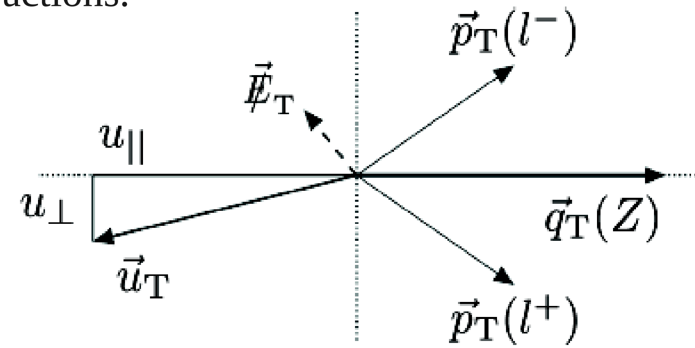

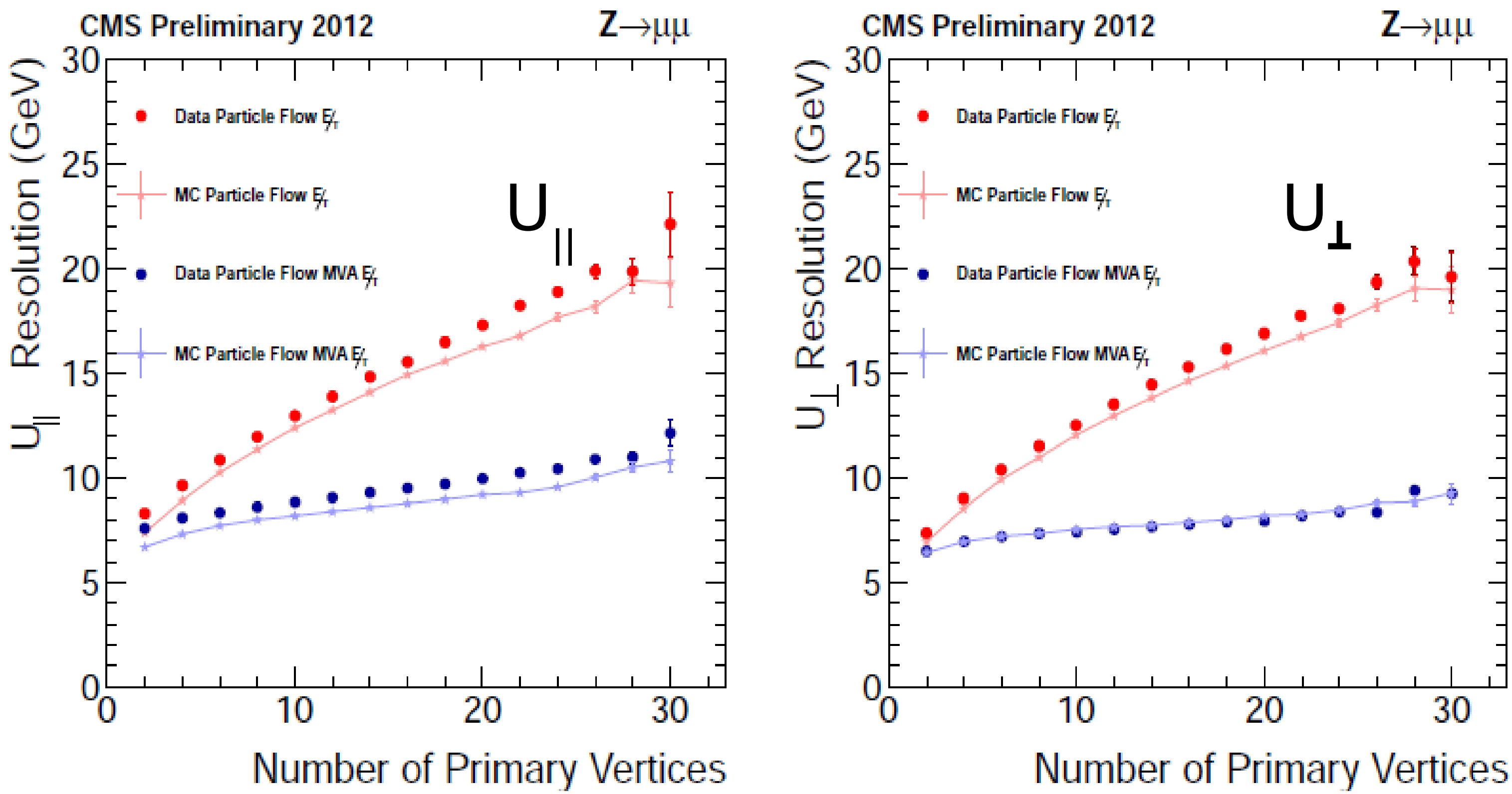

- Resolution of MVA PF E_T^{miss} is a factor of 2 better than PF E_T^{miss}

SVFit : Full di-τ mass reconstruction

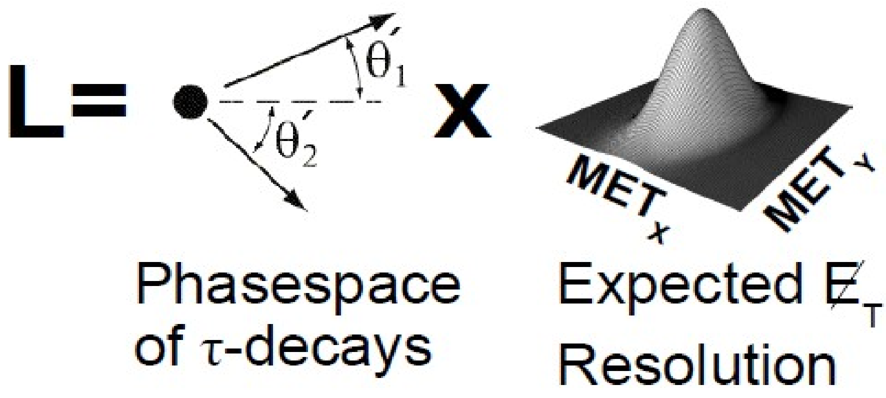

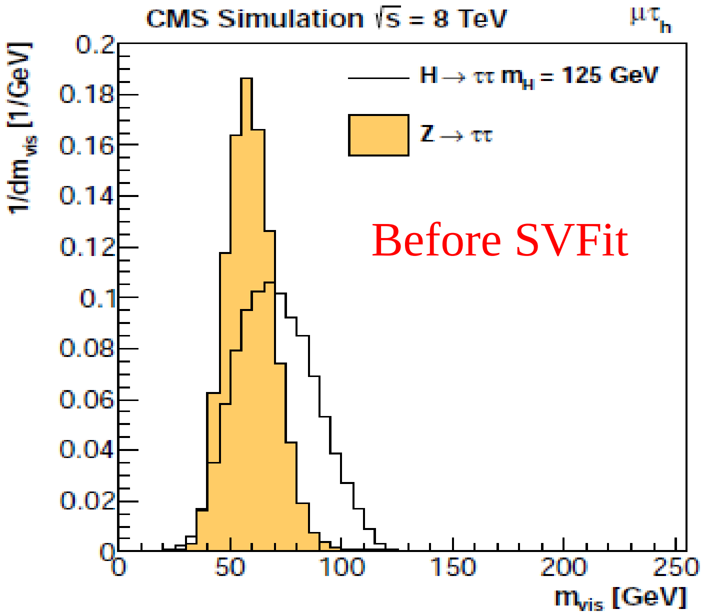

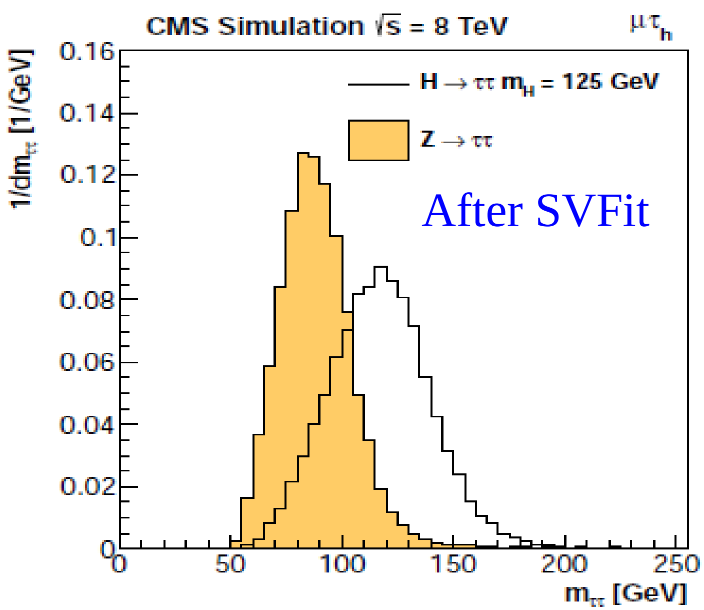

- SVFit
  - Event by event estimator of true di τ system mass (using maximum likelihood)
  - Input : four-vector information of visible leptons, x- and y-component of E_T^{miss}
- Mass peaks at true value
- Mass resolution improved by 20%
- Better separation between Higgs & Z

Analysis in a nutshell

$Z \to \tau\tau$:
- Embedding : in $Z \to \mu\mu$ replace μ by simulated τ decay
- Normalized from $Z \to \mu\mu$ events.

EWK :
- Mainly W+Jets, measured from high M_T sideband

ttbar :
- From simulations.
- Normalisation from sideband.

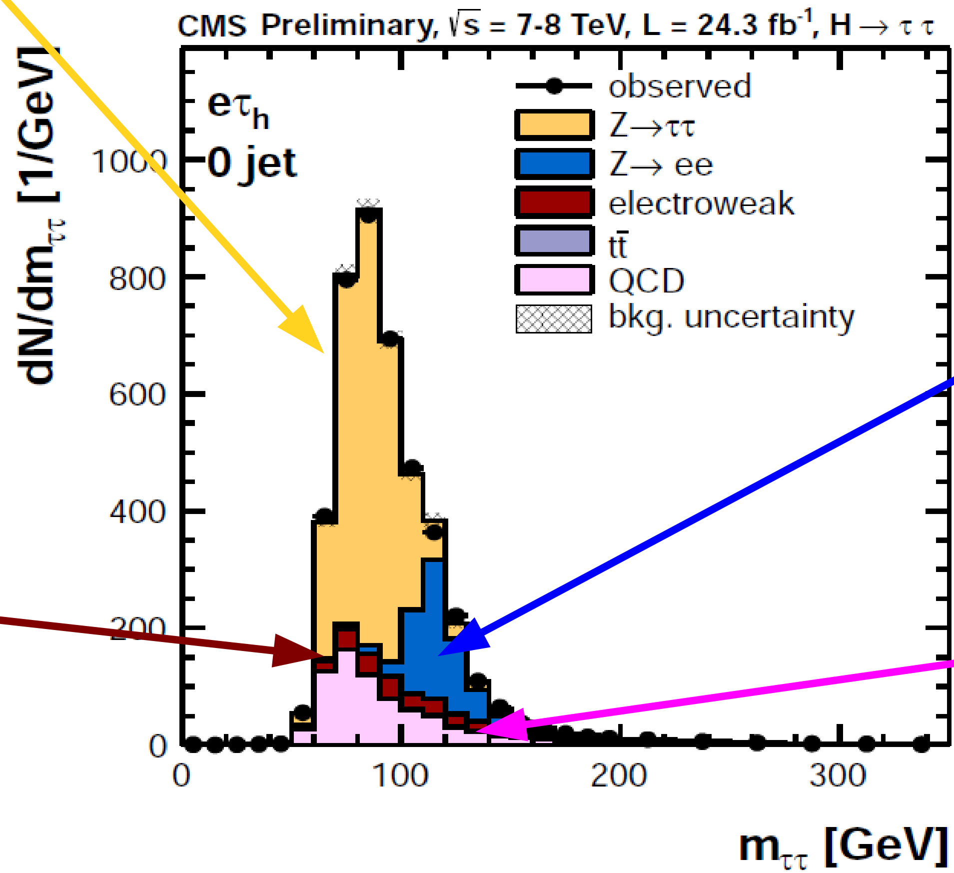

$Z \to ee/\mu\mu$:
- From simulations.
- Corrected for measured $l \to \tau$ fake rate

QCD :
- Estimated from SS data

- Final states
- $e\tau_h$ $\mu\mu$ $\mu\tau_h$ $e\mu$ $\tau_h\tau_h$

Discriminating variables

To Reject W+Jets in $e\tau_h$ & $\mu\tau_h$ channels

$$m_T = \sqrt{2 p_T E_T^{miss} (1 - \cos(\Delta\phi))}$$

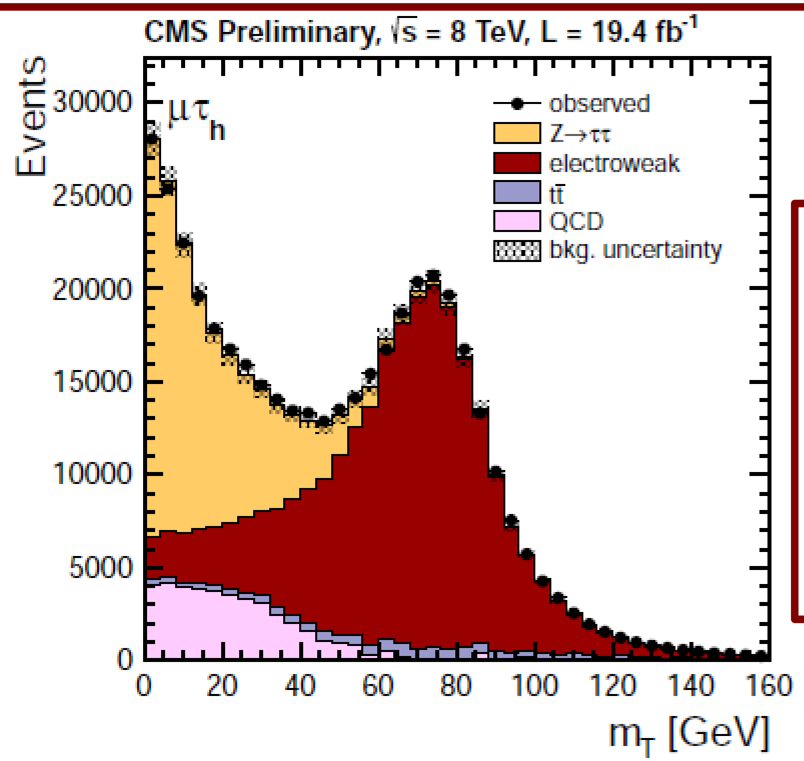

To Reject W+Jets in eμ channel

$$D_\zeta \equiv \not{p}_\zeta - 0.85 \cdot p_\zeta^{vis} > -20 \text{ GeV, where}$$
$$\not{p}_\zeta = \vec{p}_{T,1} \cdot \hat{\zeta} + \vec{p}_{T,2} \cdot \hat{\zeta} + \vec{E}_T^{miss} \cdot \hat{\zeta},$$
$$p_\zeta^{vis} = \vec{p}_{T,1} \cdot \hat{\zeta} + \vec{p}_{T,2} \cdot \hat{\zeta}.$$

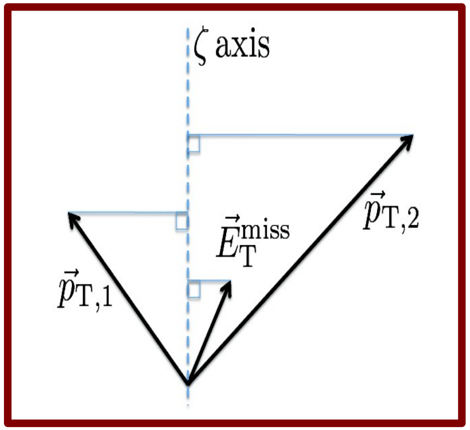

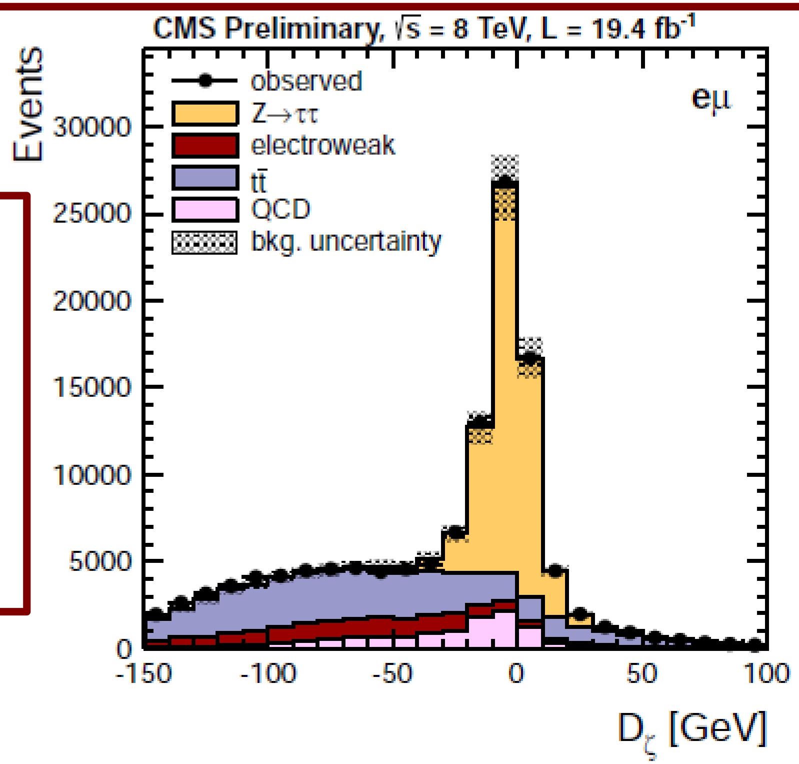

Event categories

0 Jet	0 Jet, low p_T, p_T(lepton) < 40 GeV	0 Jet, high p_T, p_T(lepton) > 40 GeV	No attempt to extract signal from this category
1 Jets	1 Jet, low p_T, p_T(lepton) < 40 GeV. Large statistics	1 Jet, high p_T, p_T(lepton) < 40 GeV. Less $Z\rightarrow\tau\tau$ background	Suppression of background from $Z\rightarrow\tau\tau$
2 Jets/VBF	2 Jet, VBF, Mjj > 500 GeV , $|\delta\eta|$ > 3.5, Central Jet veto : no jetp_T > 30 GeV		Most sensitive category

- *Fit all categories simultaneously using $M_{\tau\tau}$ templates to determine the limit following the asymptotic prescritption*

1-jets

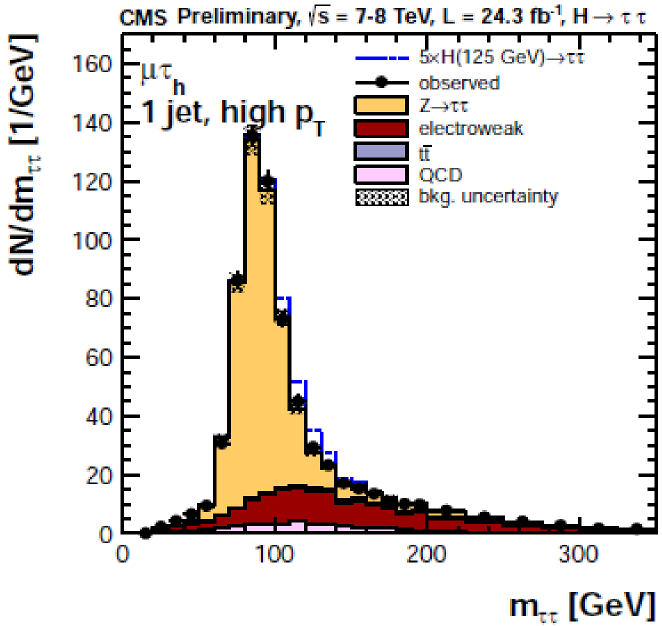

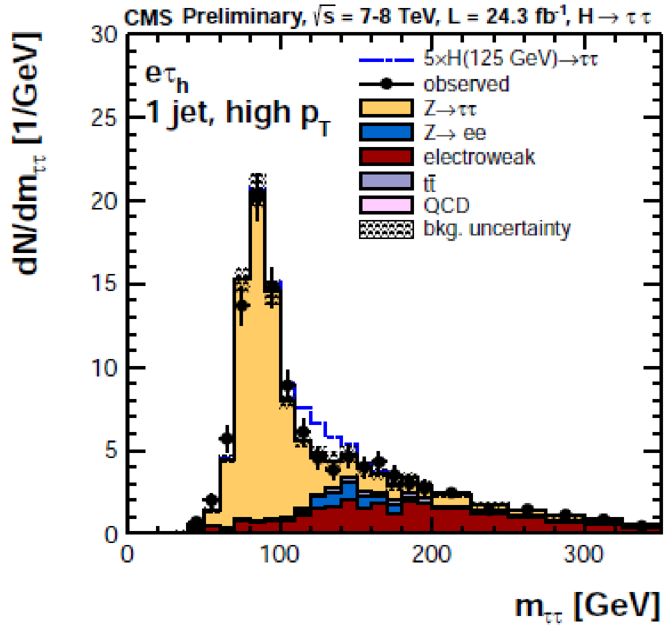

- Harder lepton p_T spectrum because of additional jet
- Signal dominating category

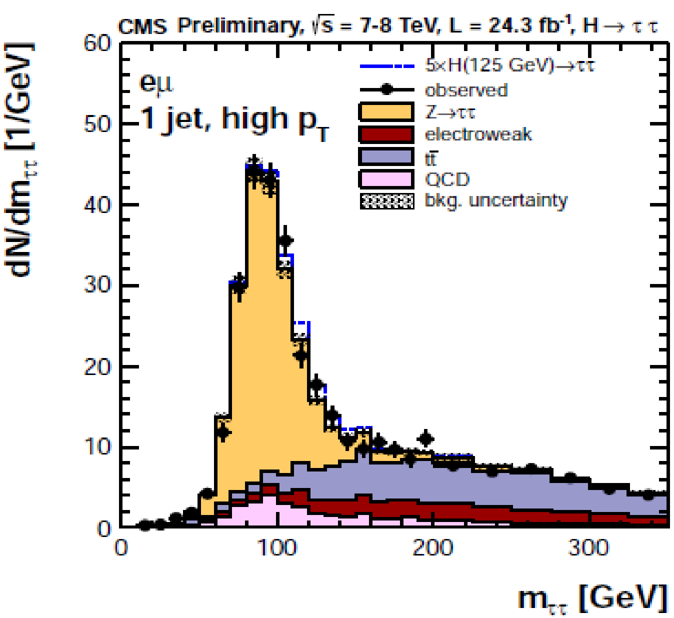

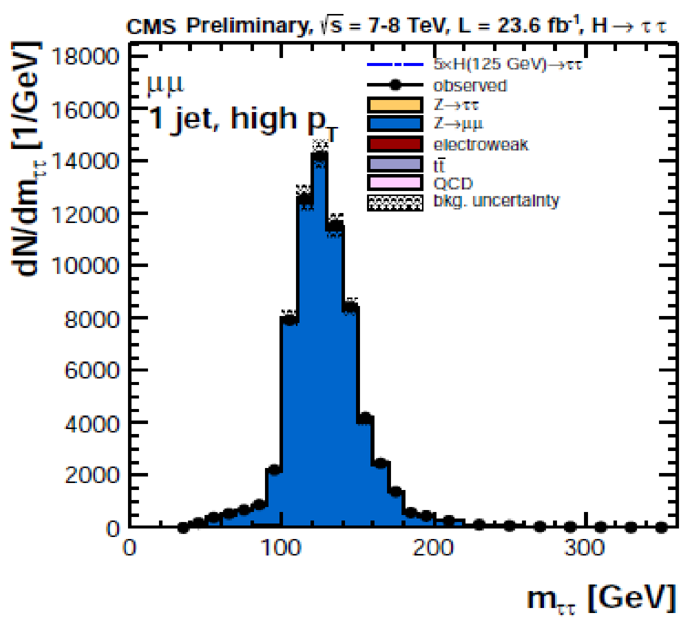

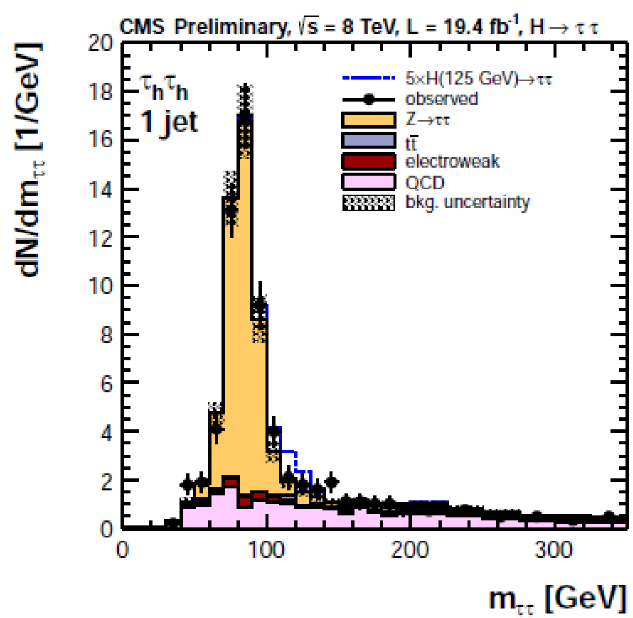

VBF

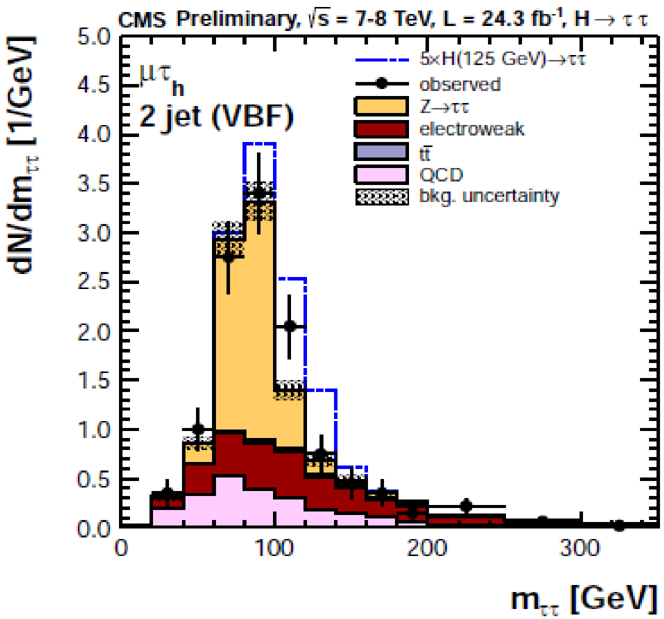

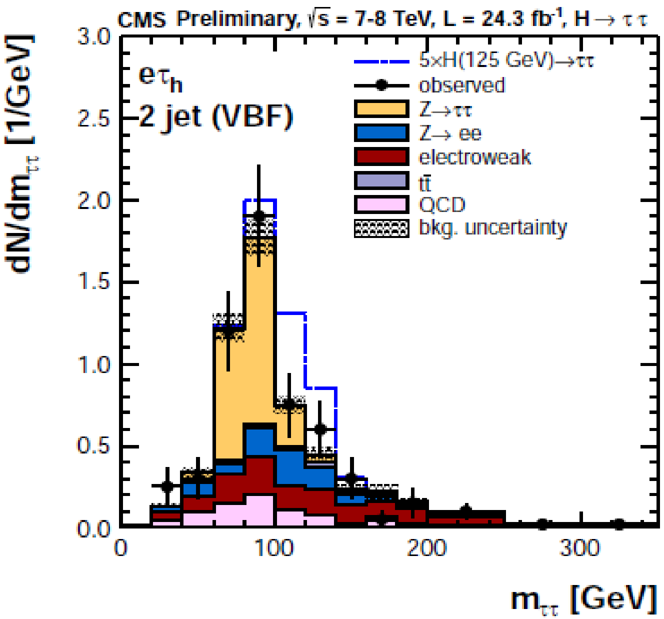

- Two jets with |δη| > 3.5
- No other jet with p_T > 30 GeV within tagged jets

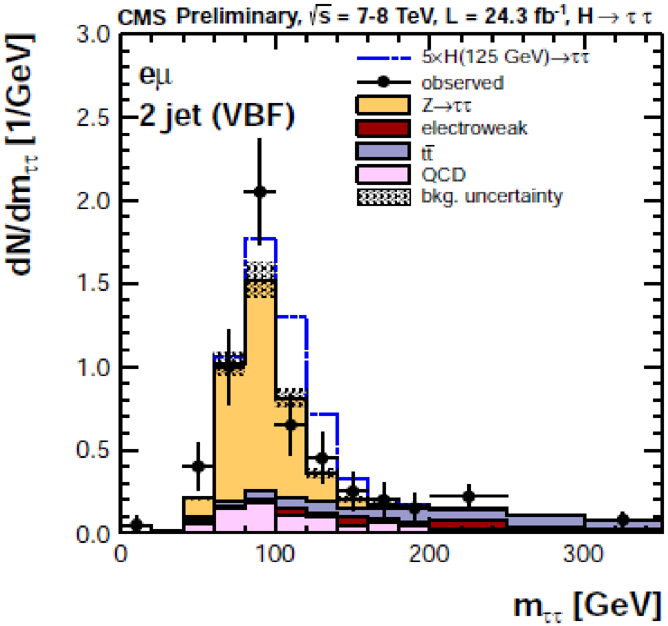

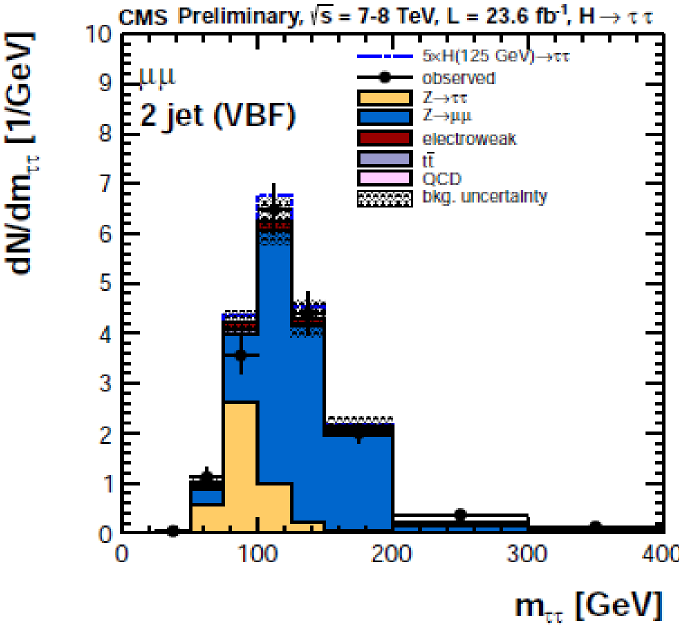

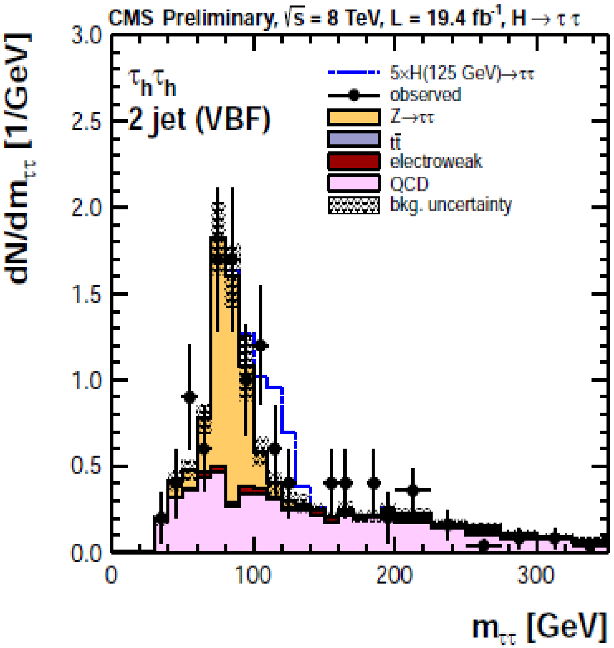

Associated production

- Higgs produced in association with W/Z boson
- Small background wrt inclusive $H \rightarrow \tau\tau$.
- Signal extracted from mass of visible decay products.

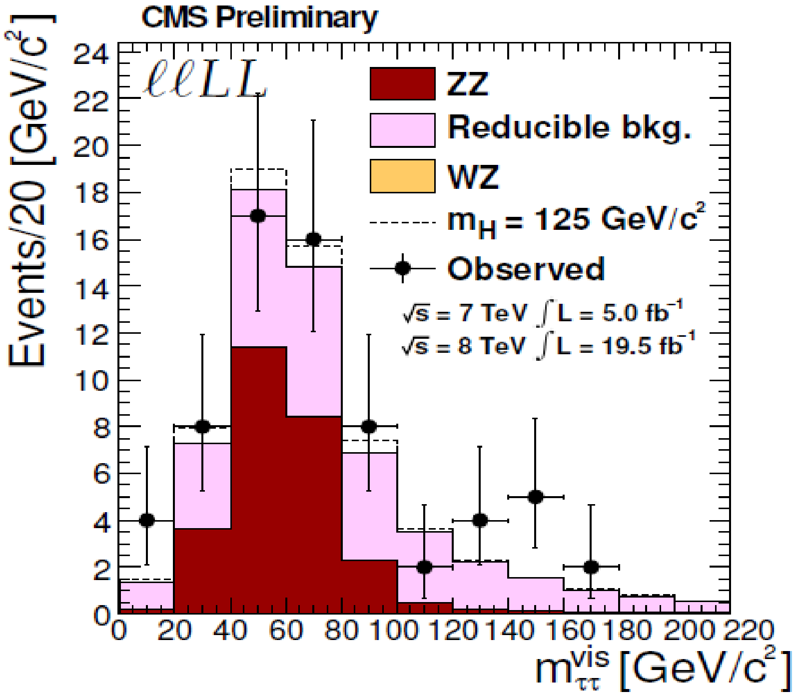

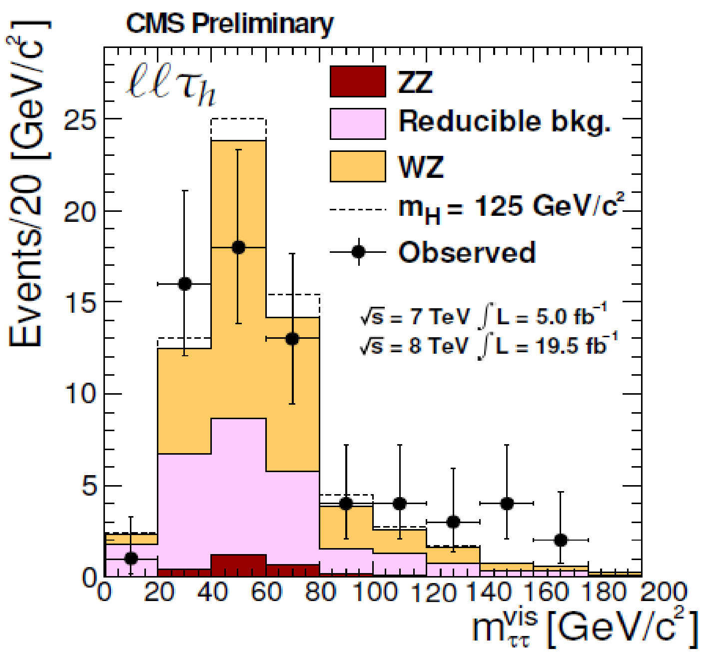

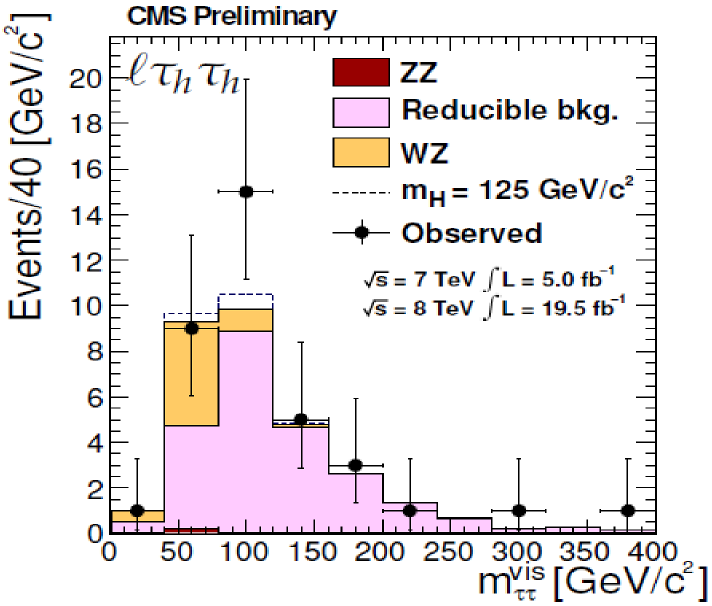

Sensitivity per Event Category & Decay channel

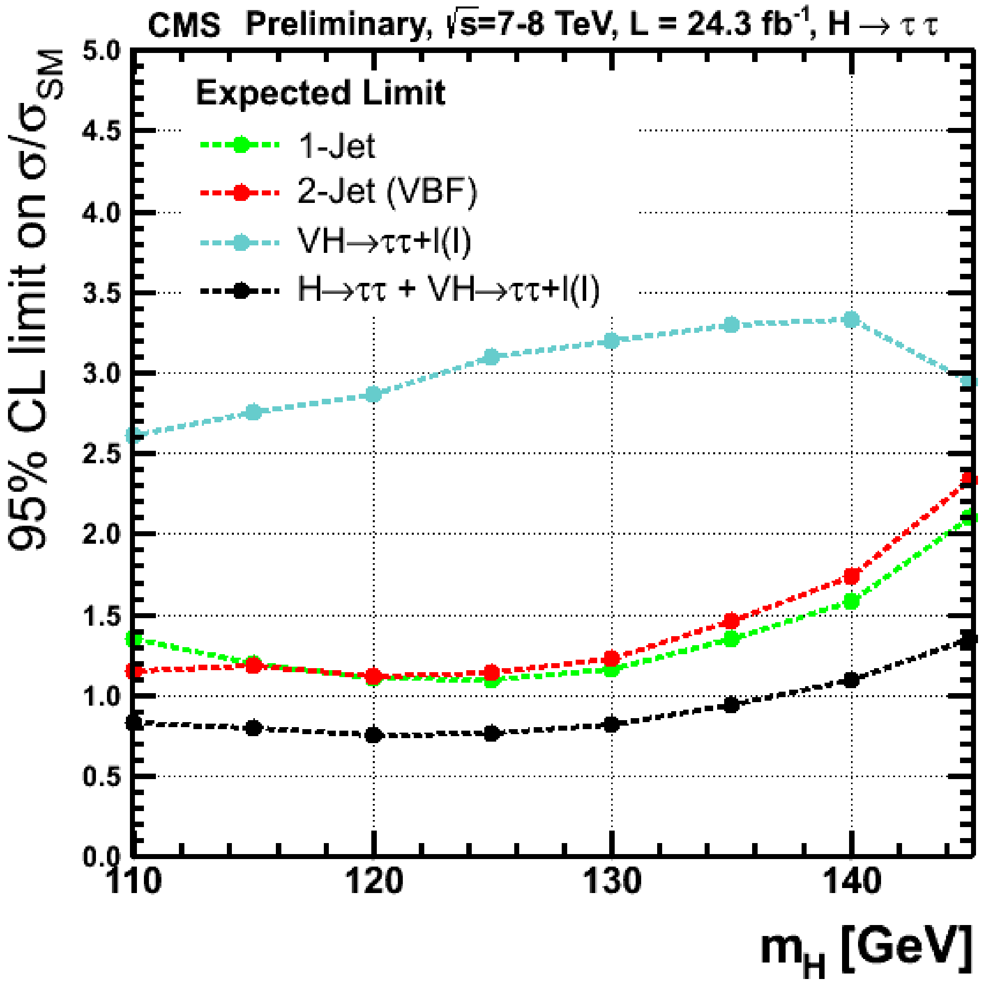

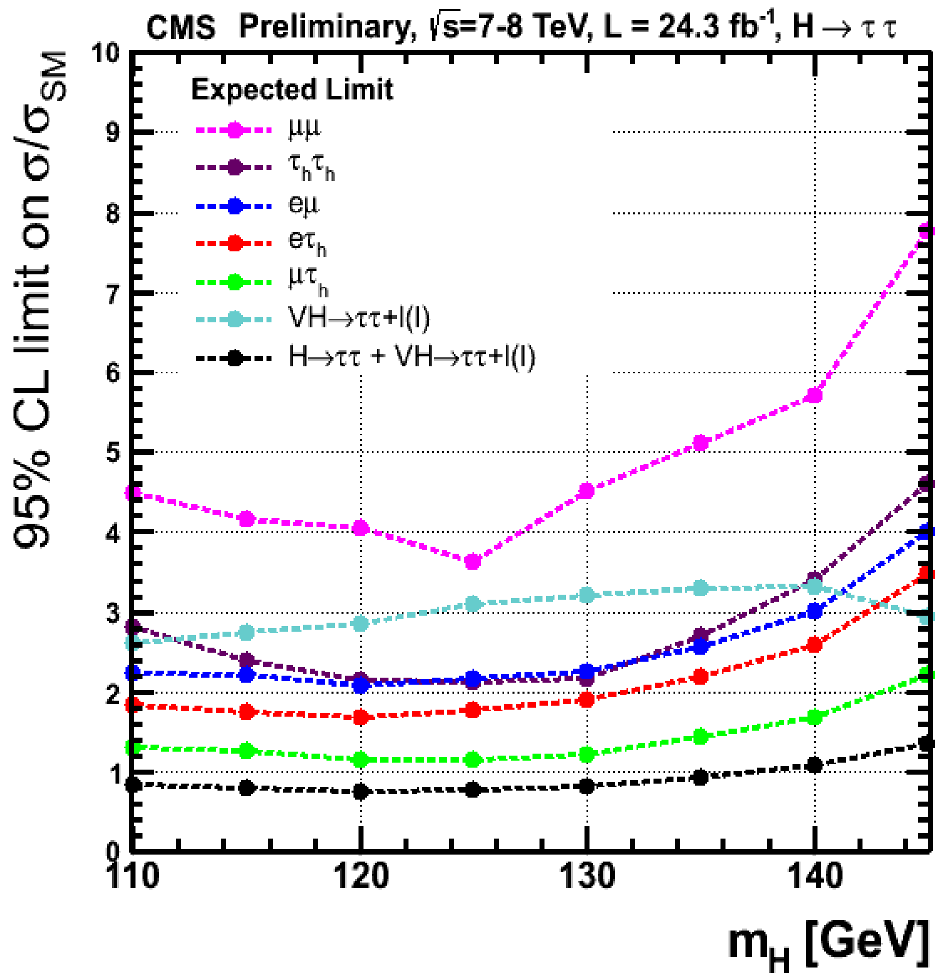

- VBF & 1-jet category roughly of equal strength at m_H = 125 GeV.
- $\mu\tau_h$ is the strongest channel.

Results

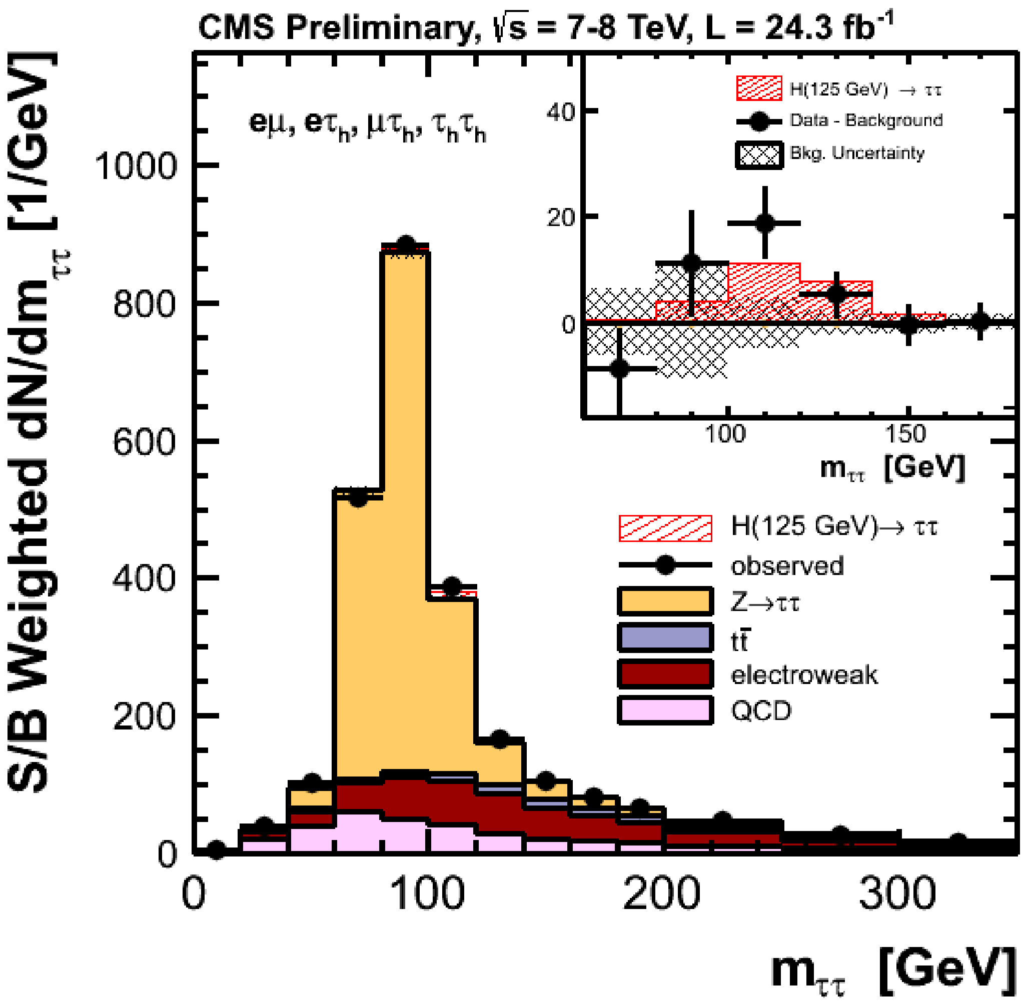

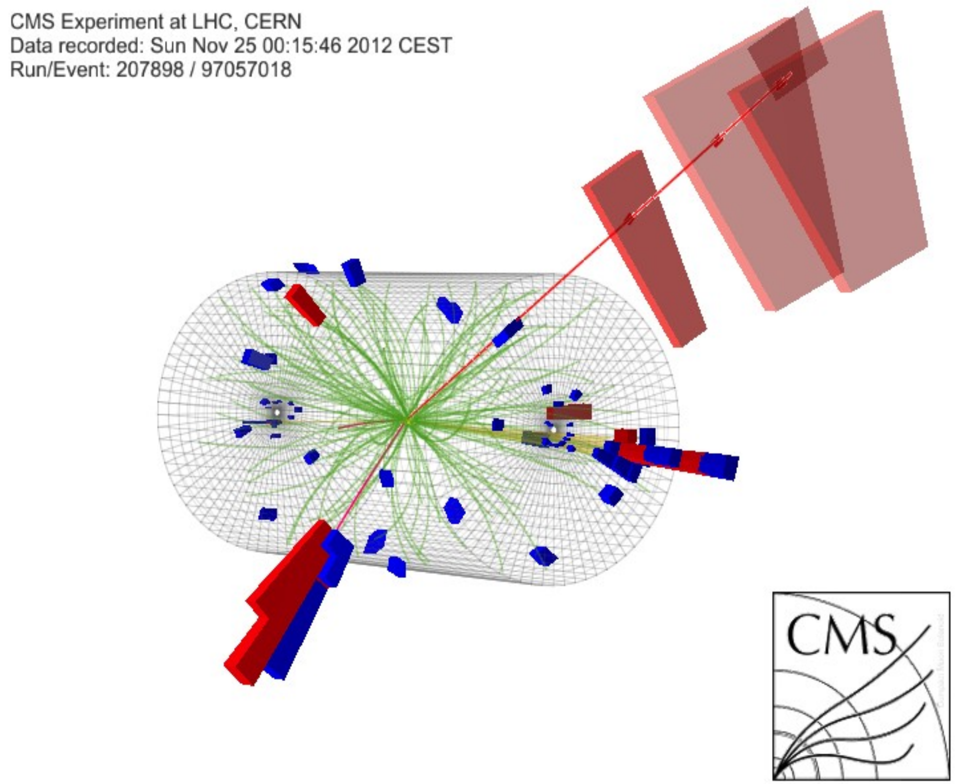

- Broad excess in $M_{\tau\tau}$ distribution

Limit of H→ττ & VH→ττ Combined

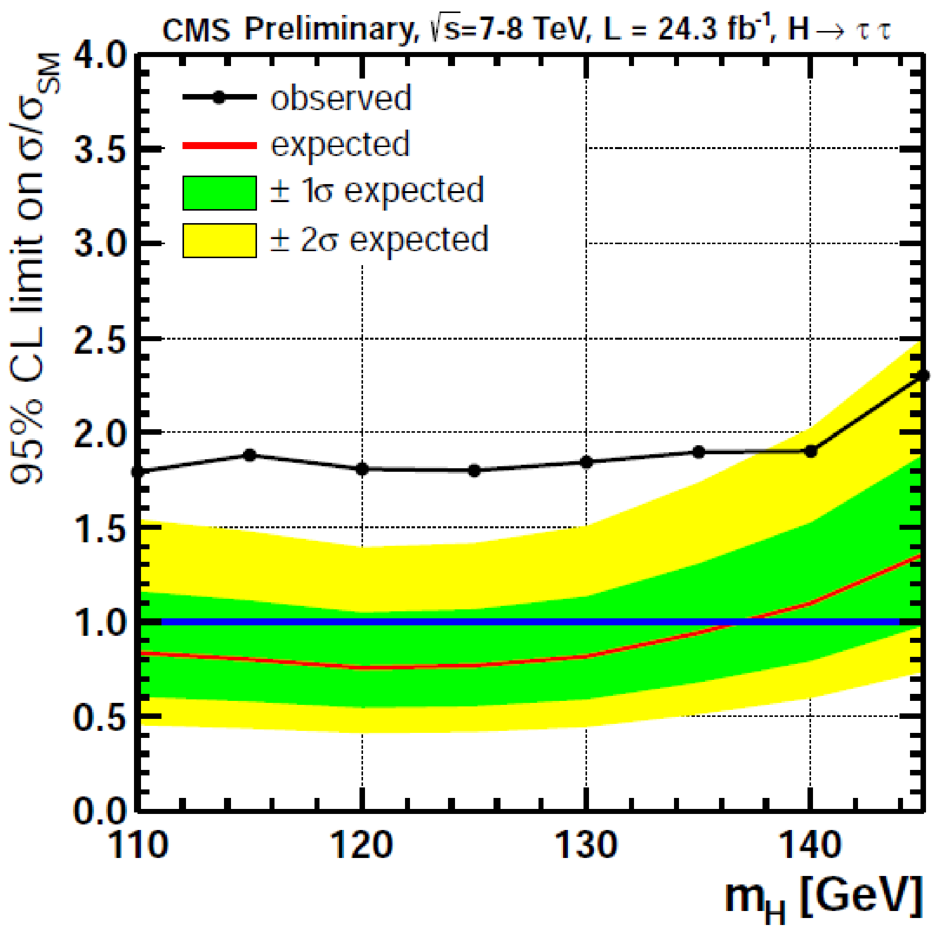

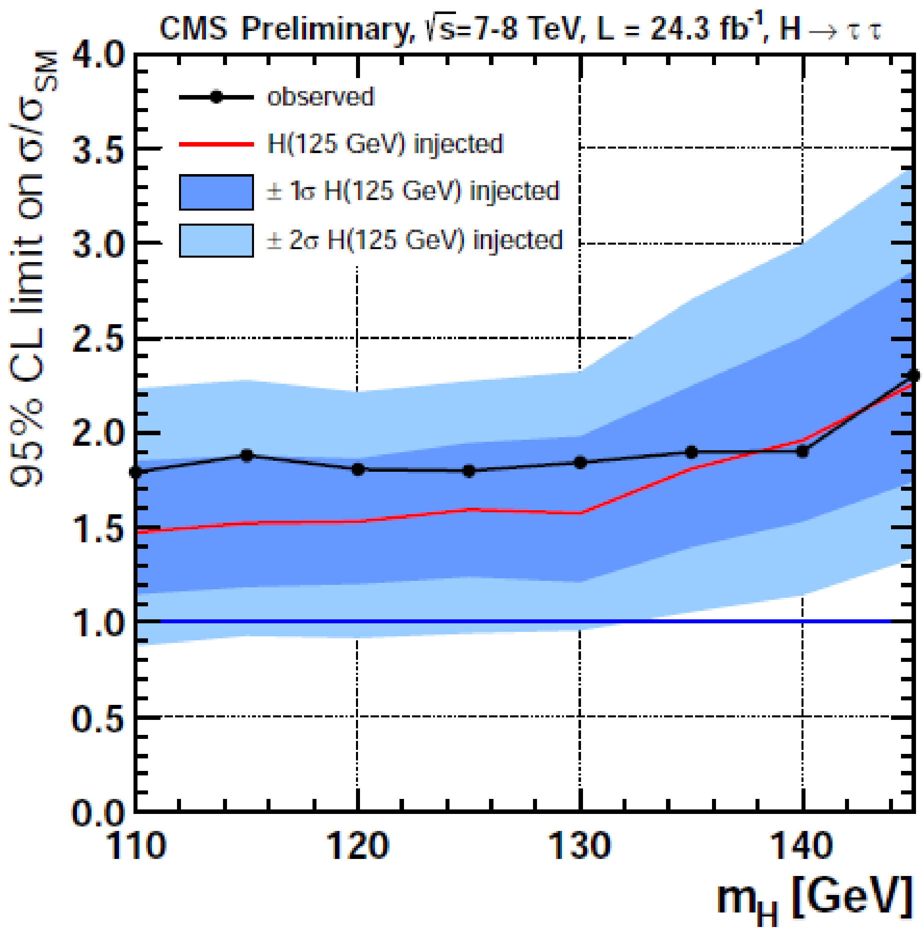

- Excess is compatible with the the presence of a SM Higgs-boson with mass m_H = 125 GeV.

p-Value

- Minimum of p-value is 2.93 σ at m_H = 120 GeV
- At m_H = 125.8 GeV, significance is 2.85 σ

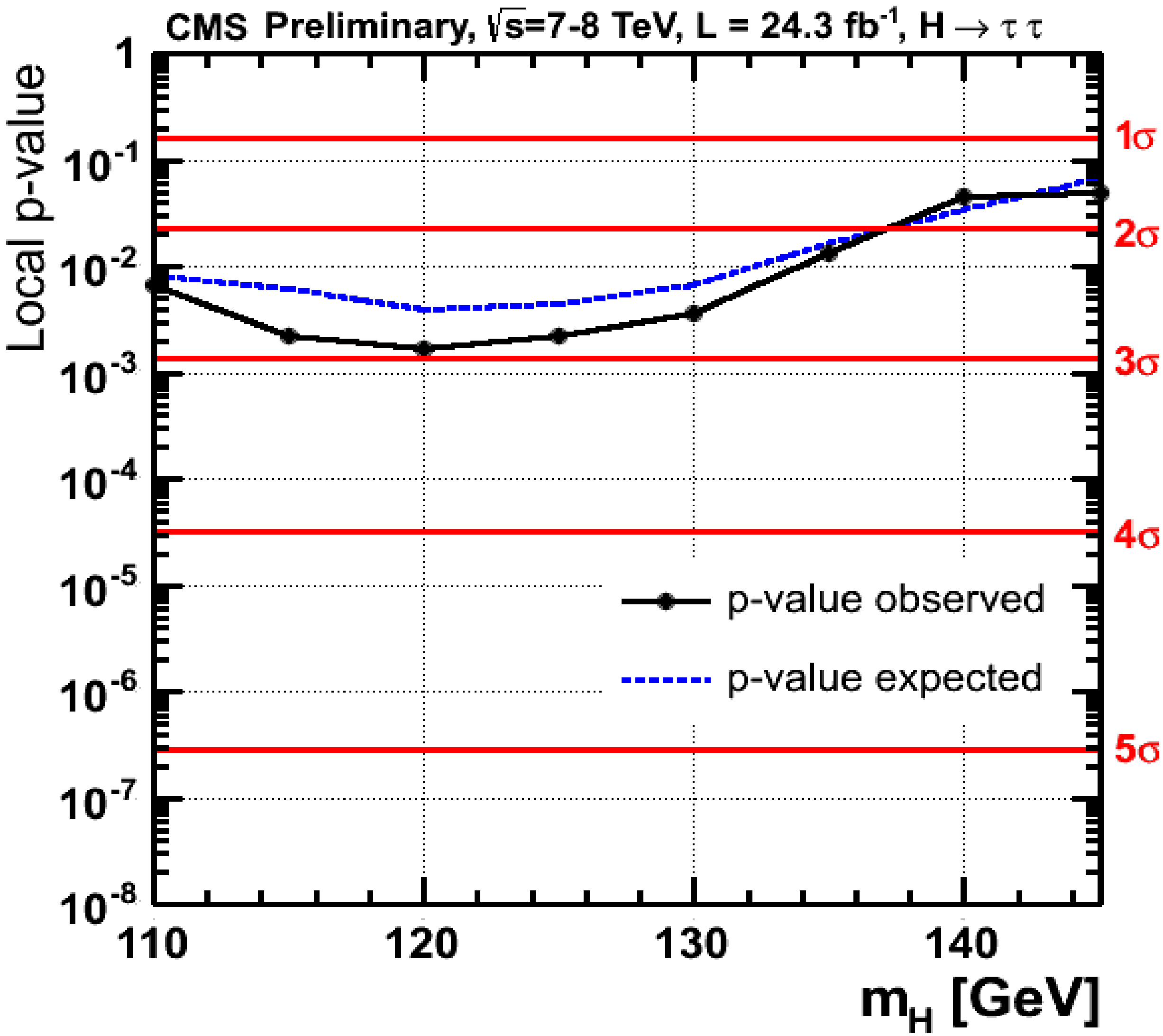

Summary

- Excess compatible with newly discovered Boson with mass 125 GeV.
- The best fit value for signal strength $\mu = 1.1 \pm 0.4$.
- New boson couples to tau leptons with a strength compatible to the one predicted by SM.

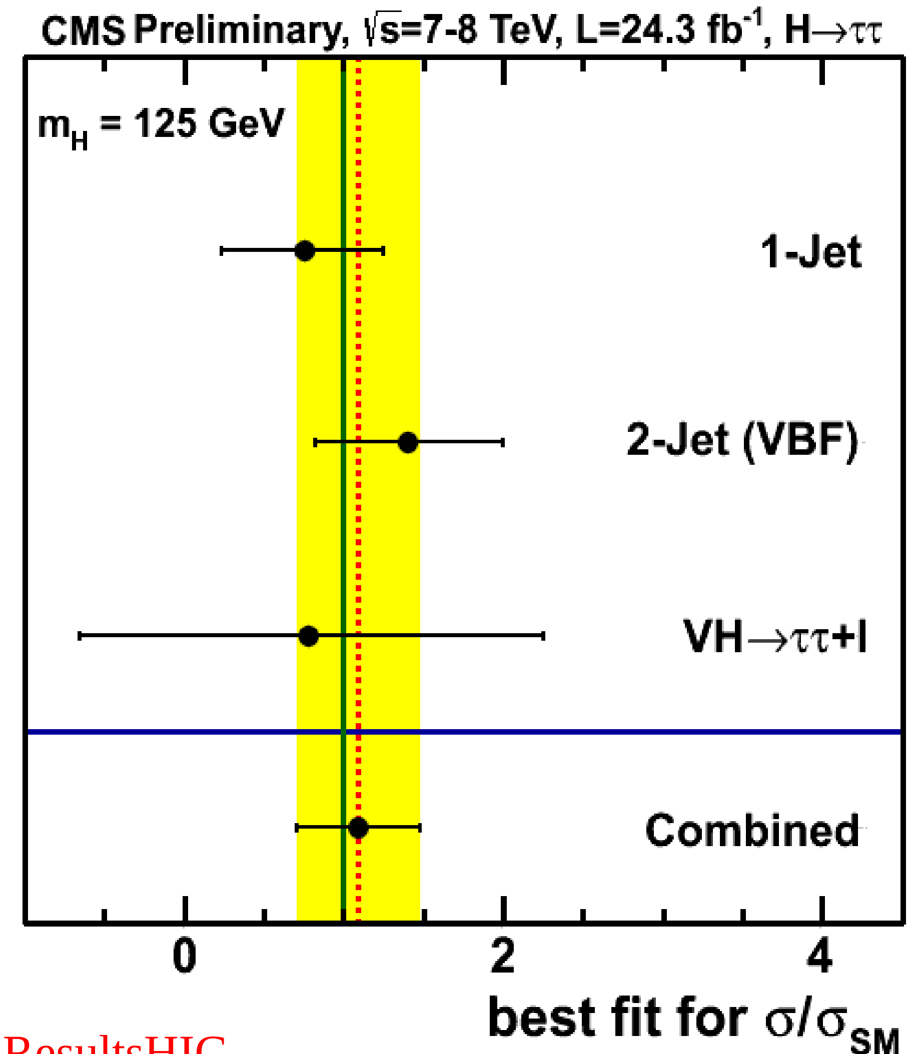

More details about analysis : HIG-12-053, HIG-13-004
https://twiki.cern.ch/twiki/bin/view/CMSPublic/PhysicsResultsHIG

Thank you

Back up slides

Cross-Section

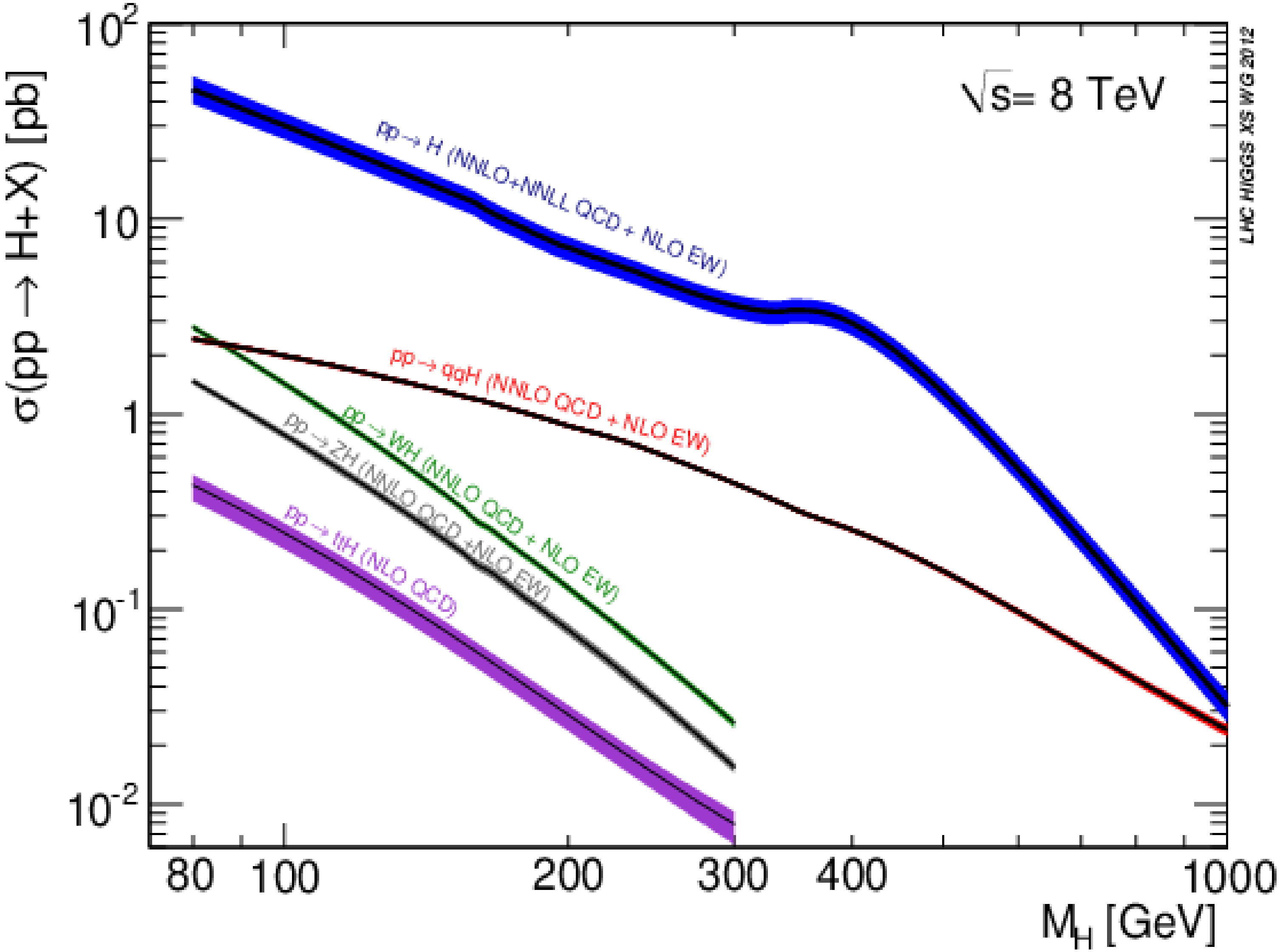

PFMET : Type 1 correction

- MET : Imbalance in the transverse momentum of all visible particles that interact via the EM or strong forces in the final state of pp collisions
- It is transverse momentum carried by weakly interacting particles, such as neutrinos.
- PFMET : The negative of vectorial sum of all PF particle transverse momentum.
- Magnitude of MET can be underestimated because of :
  - Minimum energy threshold in calorimeters.
  - Minimum p_T threshold & inefficiencies in the tracker
  - Non-linearity in the response of the calorimeter for hadronic particles.
- This is is reduced by corrected the p_T of the jets and recomputing the MET.

$$\vec{E}\!\!\!/_{\mathrm{T}}^{\mathrm{corr}} = \vec{E}\!\!\!/_{\mathrm{T}} - \sum_{\mathrm{jets}} (\vec{p}_{\mathrm{T,jet}}^{\mathrm{corr}} - \vec{p}_{\mathrm{T,jet}}),$$

PFMET : Type 0 correction

- Further corrections are applied to improve the performance of MET for events with large number of pileup interactions.
- Each pileup interaction is a minimum bias pp interaction.
- True MET is close to zero
- Vectorial sum pT of charged particles are expected to be balanced by neutral particles.
- But PFMET points in the direction of sum pT of neutral particles
  - Calorimeter non-linearity
  - Energy threshold in calorimeter for PF reconstruction.
- This is induced MET.
- Vectorial pT sum of charged particles associated to pileup vertices are used as an estimator of this induced MET, called type 0 correction.

PFMET : φ–assymetry

- Particles are produced uniformly in φ.
- Some φ asymmetry is observed pT sums of calorimeter deposits, tracks, particles reco using PF algo, leading to φ-asymmetry in MET.
- Cause can be attributed to :
  - φ-dependence of detector response
  - Imperfect allighnment of different detector sub-systems.
  - ~4mm shift between the centre of the detector & the detector beamline.
- φ–asymmetry present in both data-MC.
- Observed asymmetry is due to shift in X,Y component of MET.
  - Increases linearly with number of pile up interactions
- This corelation is used for a correction procedure.
- Linear functions are fitted and then used for correcting the MET.

PFMET : PU Independent

To construct the MVA PF $\not{E}_T$, we compute five $\vec{\not{E}}_T$ variables calculated from PF particles. These $\vec{\not{E}}_T$ variables are listed below:

- the negative vectorial sum of all PF particles in the transverse plane (PF $\vec{\not{E}}_T$),
- the negative vectorial sum of all charged PF particles that have been associated to the selected hard-scatter vertex,
- the negative vectorial sum of all charged PF particles that have been associated to the hard-scatter vertex and all neutral PF particles within jets that have passed the MVA pileup jet ID,
- the negative vectorial sum of all charged PF particles that have not been associated to the hard-scatter vertex and all neutral PF particles within jets that have failed the MVA pileup jet ID,
- the negative vectorial sum of all charged PF particles that have been associated to the hard-scatter vertex and all neutral PF particles (also those that have not been clustered into jets) plus the positive vectorial sum of all neutral PF particles within jets that have failed the MVA pileup jet ID.

0-jets

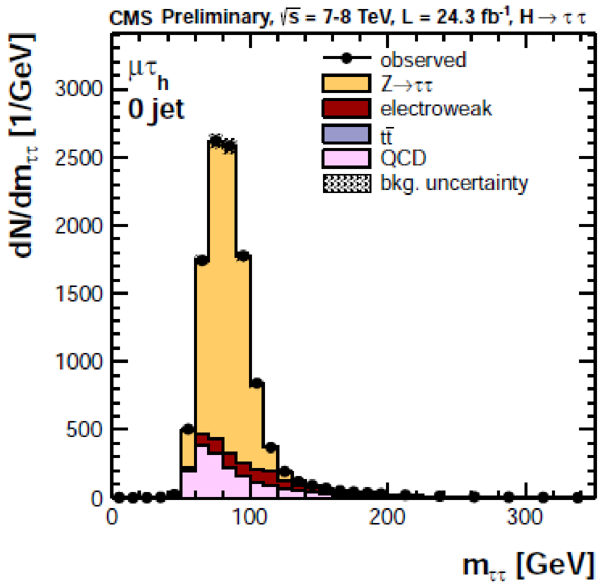

CMS Preliminary, $\sqrt{s}$ = 7-8 TeV, L = 24.3 fb^{-1}, H → τ τ
$\mu\tau_h$
0 jet
observed
Z→ττ
electroweak
$t\bar{t}$
QCD
bkg. uncertainty
dN/dm$_{\tau\tau}$ [1/GeV]
m$_{\tau\tau}$ [GeV]

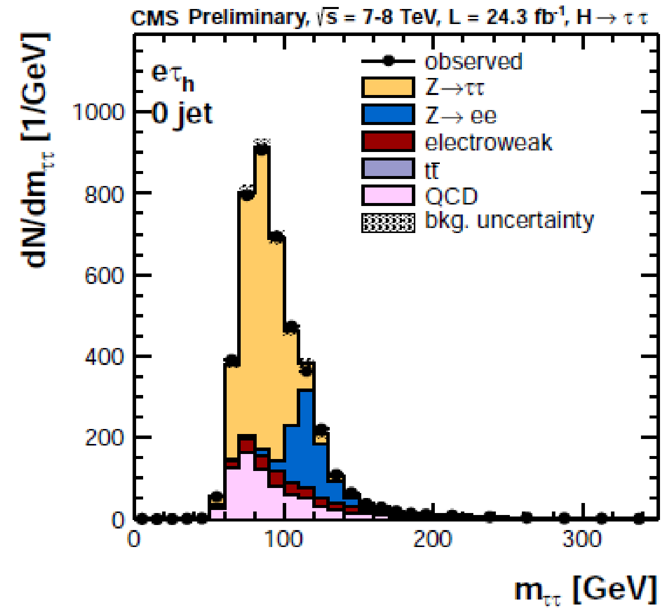

CMS Preliminary, $\sqrt{s}$ = 7-8 TeV, L = 24.3 fb^{-1}, H → τ τ
$e\tau_h$
0 jet
observed
Z→ττ
Z→ ee
electroweak
$t\bar{t}$
QCD
bkg. uncertainty
dN/dm$_{\tau\tau}$ [1/GeV]
m$_{\tau\tau}$ [GeV]

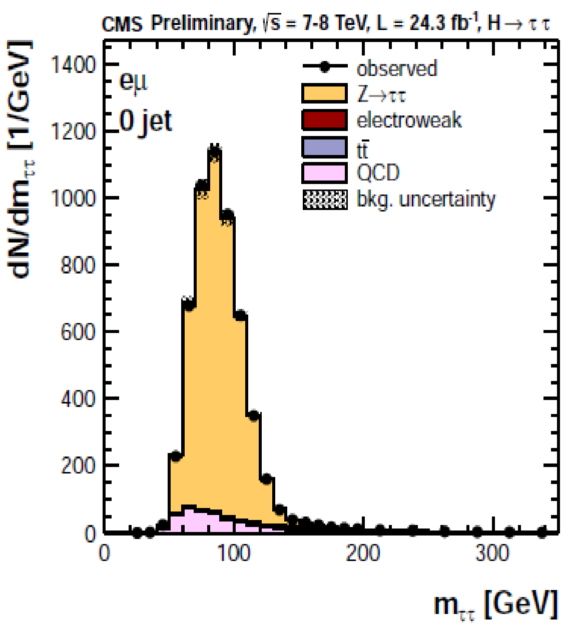

CMS Preliminary, $\sqrt{s}$ = 7-8 TeV, L = 24.3 fb^{-1}, H → τ τ
eμ
0 jet
observed
Z→ττ
electroweak
$t\bar{t}$
QCD
bkg. uncertainty
dN/dm$_{\tau\tau}$ [1/GeV]
m$_{\tau\tau}$ [GeV]

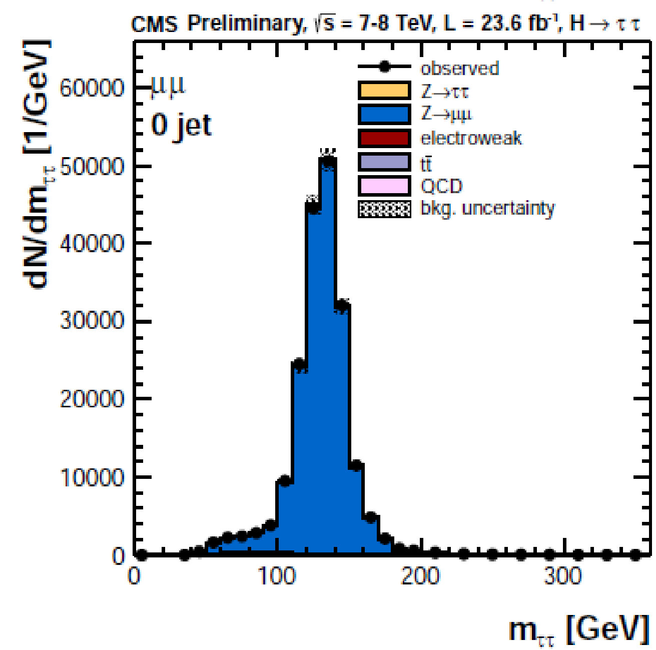

CMS Preliminary, $\sqrt{s}$ = 7-8 TeV, L = 23.6 fb^{-1}, H → τ τ
μμ
0 jet
observed
Z→ττ
Z→μμ
electroweak
$t\bar{t}$
QCD
bkg. uncertainty
dN/dm$_{\tau\tau}$ [1/GeV]
m$_{\tau\tau}$ [GeV]

Systematics : Experimental

Experimental Uncertainties		Propagation into Event Categories		
Uncertainty	Uncert.	*0-Jet*	*1-Jet*	*VBF*
Electron ID & Trigger (†*)	$\pm 2\%$	$\pm 2\%$	$\pm 2\%$	$\pm 2\%$
Muon ID & Trigger (†*)	$\pm 2\%$	$\pm 2\%$	$\pm 2\%$	$\pm 2\%$
Tau ID & Trigger (†)	$\pm 8\%$	$\pm 8\%$	$\pm 8\%$	$\pm 8\%$
Tau Energy Scale (†)	$\pm 3\%$	$\pm 3\%$	$\pm 3\%$	$\pm 3\%$
Electron Energy Scale (†)	$\pm 1\%$	$\pm 1\%$	$\pm 1\%$	$\pm 1\%$
JES (Norm.) (†*)	$\pm 2.5 - 5\%$	$\mp 3 - 15\%$	$\pm 1 - 6\%$	$\pm 5 - 20\%$
MET (Norm.) (†*)	$\pm 5\%$	$\pm 5 - 7\%$	$\pm 2 - 7\%$	$\pm 5 - 8\%$
b-Tag Efficiency (†*)	$\pm 10\%$	$\mp 2\%$	$\mp 2 - 3\%$	$\mp 3\%$
Mis-Tagging (†*)	$\pm 30\%$	$\mp 2\%$	$\mp 2\%$	$\mp 2 - 3\%$
Norm. Z production (†*)	$\pm 3\%$	$\pm 3\%$	$\pm 3\%$	$\pm 3\%$
$Z \to \tau\tau$ Category	$\pm 3\%$	$\pm 0 - 5\%$	$\pm 3 - 5\%$	$\pm 10 - 13\%$
Norm. $t\bar{t}$ (†* ex.vbf)	$\pm 10\%$	$\pm 10\%$	$\pm 10\%$	$\pm 12 - 33\%$
Norm. Diboson (†* ex. vbf)	$\pm 15 - 30\%$	$\pm 15 - 30\%$	$\pm 15 - 30\%$	$\pm 15 - 100\%$
Norm. QCD Multijet	$\pm 6 - 32\%$	$\pm 6 - 32\%$	$\pm 9 - 30\%$	$\pm 19 - 35\%$
Lumi 7 TeV (8 TeV)	$\pm 2.2(4.2)\%$	$\pm 2.2(4.2)\%$	$\pm 2.2(4.2)\%$	$\pm 2.2(4.2)\%$
Norm. W+jets	$\pm 10 - 30\%$	$\pm 20 - 27\%$	$\pm 10 - 33\%$	$\pm 12.4\% - 30\%$
Norm. $Z \to \ell\ell$: e fakes τ_h (†)	$\pm 20\%$	$\pm 20\%$	$\pm 36\%$	$\pm 22\%$
Norm. $Z \to \ell\ell$: μ fakes τ_h (†)	$\pm 30\%$	$\pm 30\%$	$\pm 30\%$	$\pm 30\%$
Norm. $Z \to \ell\ell$: jet fakes τ_h	$\pm 20\%$	$\pm 20\%$	$\pm 20\%$	$\pm 40\%$

Systematics : Theoritical

Theory Uncertainties (SM)		Propagation into Limit Calculation		
Uncertainty	Uncert.	*0-Jet*	*1-Jet*	*VBF*
PDF (†*)	-	-	$\pm 2-8\%$	$\pm 2-8\%$
$\mu_r/\mu_f(gg \to H)$ (†*)	-	-	$\pm 10\%$	$\pm 30\%$
$\mu_r/\mu_f(qq \to H)$ (†*)	-	-	$\pm 4\%$	$\pm 4\%$
$\mu_r/\mu_f(qq \to VH)$ (†*)	-	-	$\pm 4\%$	$\pm 4\%$
UE & PS (†*)	-	-	$\pm 4\%$	$\pm 4\%$

Event Yield Table

Observed and expected event yields, and expected signal efficiency in the $\mu\tau_h$ channel.

Process	*0-Jet*	*1-Jet high* p_T	*VBF*
$Z\rightarrow \tau\tau$	84833 ± 1927	4686 ± 232	109 ± 11
QCD	18313 ± 478	481 ± 38	48 ± 7
EWK	8841 ± 653	1585 ± 153	63 ± 9
$t\bar{t}$	11 ± 1	155 ± 11	5 ± 1
Total Background	111998 ± 2090	6908 ± 281	225 ± 16
$H\rightarrow \tau\tau$	- ± -	73 ± 13	11 ± 2
Observed	112279	7011	240

Signal Eff.

$gg\rightarrow H$	-	$1.99 \cdot 10^{-3}$	$8.51 \cdot 10^{-5}$
$qq\rightarrow H$	-	$4.09 \cdot 10^{-3}$	$3.46 \cdot 10^{-3}$
$qq\rightarrow Ht\bar{t}$ or VH	-	$3.00 \cdot 10^{-3}$	$1.60 \cdot 10^{-5}$

Event Yield Table

Observed and expected event yields, and expected signal efficiency in the $e\tau_h$ channel.

Process	*0-Jet*	*1-Jet high p_T*	*VBF*
Z→ $\tau\tau$	25161 ± 708	792 ± 62	47 ± 6
QCD	7706 ± 307	3 ± 0.3	17 ± 4
EWK	9571 ± 510	365 ± 53	44 ± 6
$t\bar{t}$	4 ± 0.5	47 ± 4	4 ± 1
Total Background	42443 ± 924	1207 ± 82	113 ± 9
H→ $\tau\tau$	- ± -	15 ± 3	5 ± 1
Observed	42481	1217	117

Signal Eff.

gg→ H	-	$3.94 \cdot 10^{-4}$	$3.33 \cdot 10^{-5}$
qq→ H	-	$1.10 \cdot 10^{-3}$	$1.78 \cdot 10^{-3}$
qq→ H$t\bar{t}$ or VH	-	$8.30 \cdot 10^{-4}$	$1.46 \cdot 10^{-6}$

Event Yield Table

Observed and expected event yields, and expected signal efficiency in the $\tau_h \tau_h$ channel.

Process	*1-Jet*	*VBF*
$Z \rightarrow \tau\tau$	428 ± 90	47 ± 28
QCD	210 ± 31	61 ± 10
EWK	41 ± 9	4 ± 1
$t\bar{t}$	29 ± 6	2 ± 2
Total Background	709 ± 95	114 ± 30
$H \rightarrow \tau\tau$	9 ± 4	4 ± 2
Observed	718	120

Signal Eff.

$gg \rightarrow H$	$2.52 \cdot 10^{-4}$	$4.99 \cdot 10^{-5}$
$qq \rightarrow H$	$5.93 \cdot 10^{-4}$	$1.20 \cdot 10^{-3}$
$qq \rightarrow Ht\bar{t}$ or VH	$9.13 \cdot 10^{-4}$	$3.59 \cdot 10^{-5}$

Event Yield Table

Observed and expected event yields, and expected signal efficiency in the eμ channel.

Process	*0-Jet*	*1-Jet high p_T*	*VBF*
Z$\rightarrow \tau\tau$	48882 ± 1282	1830 ± 105	61 ± 6
QCD	4374 ± 249	395 ± 36	19 ± 2
EWK	1185 ± 89	461 ± 44	7 ± 1
$t\bar{t}$	74 ± 5	1100 ± 66	19 ± 2
Total Background	54514 ± 1309	3785 ± 137	105 ± 7
H$\rightarrow \tau\tau$	- $\pm$ -	23 ± 4	5 ± 0.6
Observed	54694	3774	118

Signal Eff.

gg$\rightarrow$ H	-	$6.04 \cdot 10^{-4}$	$3.27 \cdot 10^{-5}$
qq$\rightarrow$ H	-	$1.37 \cdot 10^{-3}$	$1.80 \cdot 10^{-3}$
qq$\rightarrow$ H$t\bar{t}$ or VH	-	$1.38 \cdot 10^{-3}$	$1.32 \cdot 10^{-5}$

Event Yield Table

Observed and expected event yields, and expected signal efficiency in the $\mu\mu$ channel.

Process	*0-Jet*	*1-Jet high p_T*	*VBF*
$Z \to \mu\mu$	1925174 ± 52051	685272 ± 27303	380 ± 38
$Z \to \tau\tau$	20669 ± 470	3888 ± 157	116 ± 9
QCD	1299 ± 226	561 ± 161	6 ± 11
EWK	4732 ± 1594	7827 ± 1297	22 ± 9
$t\bar{t}$	4708 ± 2110	2168 ± 522	15 ± 5
Total Background	1956582 ± 52120	699717 ± 27418	539 ± 42
$H \to \tau\tau$	- ± -	37 ± 5	5 ± 1
Observed	1956931	700020	548

Signal Eff.

$gg \to H$	-	$9.50 \cdot 10^{-4}$	$7.23 \cdot 10^{-5}$
$qq \to H$	-	$1.85 \cdot 10^{-3}$	$1.03 \cdot 10^{-3}$
$qq \to Ht\bar{t}$ or VH	-	$2.95 \cdot 10^{-3}$	$1.39 \cdot 10^{-4}$

Limit value

SM Higgs	Expected limit								
m_H	-2σ	-1σ	Median	$+1\sigma$	$+2\sigma$	Obs. Limit	Obs. 1-CL_b	Exp. Sig.	Obs Sig.
110 GeV	0.45	0.60	0.84	1.16	1.54	1.79	0.0067	2.4	2.47
115 GeV	0.43	0.58	0.80	1.11	1.48	1.88	0.0023	2.5	2.84
120 GeV	0.41	0.55	0.76	1.05	1.39	1.81	0.0017	2.65	2.93
125 GeV	0.42	0.55	0.77	1.07	1.42	1.80	0.0022	2.62	2.85
130 GeV	0.44	0.59	0.82	1.13	1.51	1.84	0.0037	2.47	2.68
135 GeV	0.51	0.68	0.94	1.31	1.74	1.90	0.0135	2.12	2.21
140 GeV	0.60	0.79	1.10	1.52	2.03	1.90	0.0457	1.83	1.69
145 GeV	0.74	0.98	1.36	1.88	2.50	2.30	0.0487	1.49	1.66

Result

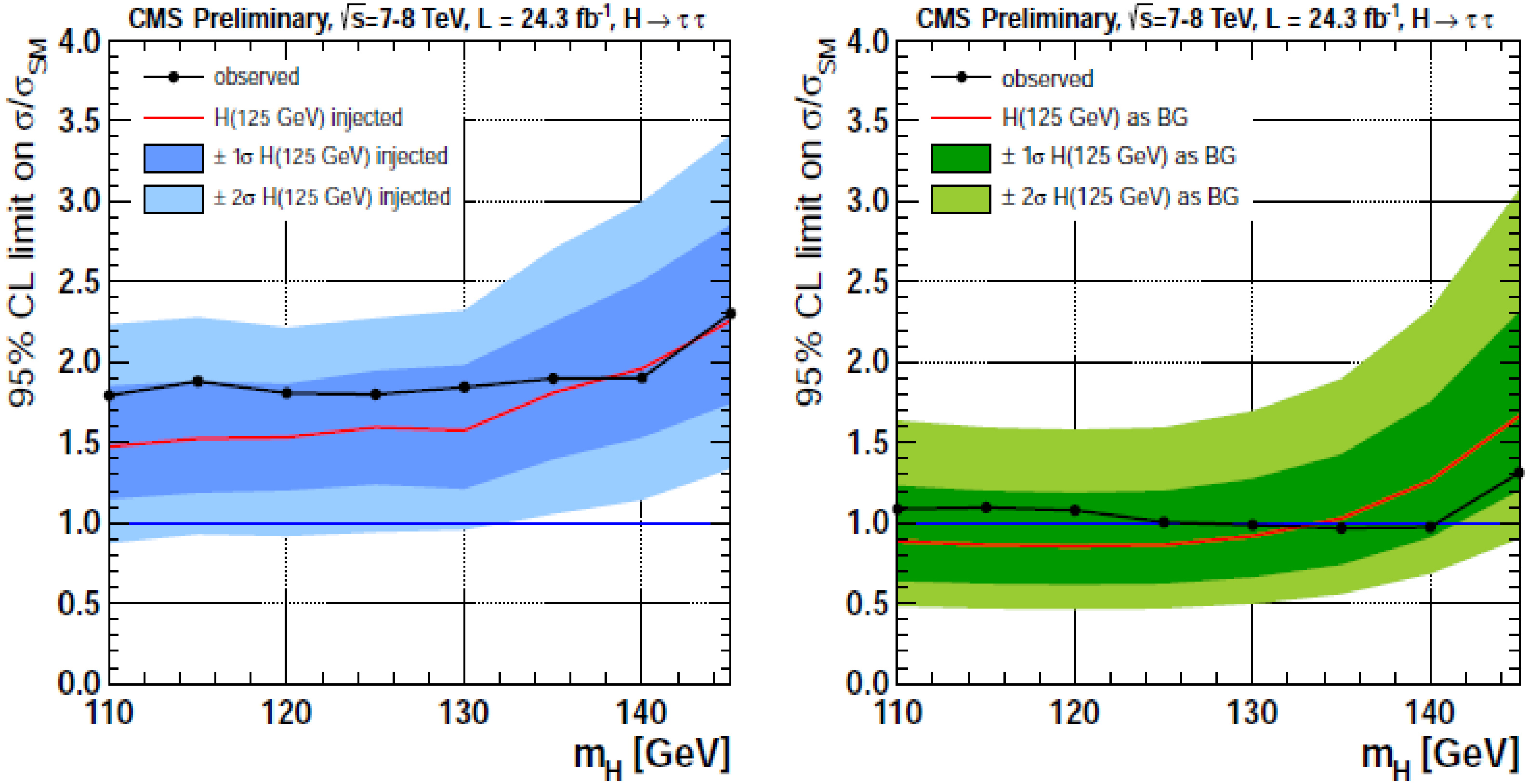

Combined observed 95% CL upper limit on the signal strength parameter $\mu = \sigma/\sigma_{\mathrm{SM}}$, together with the expected limit obtained in the background hypothesis (top), the signal plus background hypothesis for a SM Higgs boson with $m_{\mathrm{H}} = 125$ GeV (bottom left), and a background hypothesis including this SM Higgs boson signal as a background (bottom right). The bands show the expected one- and two-standard-deviation probability intervals around the expected limit. These results include the search for a SM Higgs boson decaying into a τ pair and produced in association with a W or Z boson decaying leptonically.

Best Fit : each channel